Available online at www.sciencedirect.com
SCIENCE DIRECT
International Journal of Mass Spectrometry 245 (2005) 78–89
International Journal of Mass Spectrometry
www.elsevier.com/locate/ijms

On-line analysis of organic compounds in diesel exhaust using a proton transfer reaction mass spectrometer (PTR-MS)

B.T. Jobson *, M.L. Alexander, G.D. Maupin, G.G. Muntean

Battelle Pacific Northwest, P.O. Box 999, Richland, WA, USA

Received 22 March 2005; received in revised form 27 May 2005; accepted 27 May 2005
Available online 19 August 2005

Abstract

Chemical ionization mass spectrometry using H_3O^+ proton transfer in an ion drift tube (PTR-MS) was used to measure volatile organic compound (VOC) concentrations on-line in diesel engine exhaust as a function of engine load. The purpose of the study was to evaluate the PTR-MS instrument as an analytical tool for diesel engine emissions abatement research. Measured sensitivities determined from gas standards were found to agree well with calculated sensitivities for non-polar species. A slight humidity dependent sensitivity was observed for non-polar species, implying that reactions with $H^+(H_2O)_2$ were important for some organics. The diesel exhaust mass spectra were complex but displayed a pattern of strong ion signals at $14n + 1$ ($n = 3.8$) masses, with a relative ion abundance similar to that obtained from electron impact ionization of alkanes. Laboratory experiments verified that C_8–C_{16} *n*-alkanes and C_8–C_{13} 1-alkenes react with H_3O^+ in dissociative proton transfer reaction resulting in alkyl cation ion products, primarily *m*/*z* 41, 43, 57, 71 and 85. Monitoring the sum of these ion signals may be useful for estimating alkane emissions from unburnt diesel fuel. Alkane fragmentation likely simplified the diesel exhaust mass spectrum and reduced potential mass interferences with isobaric aromatic compounds. Concentrations of aldehydes and ketones dominated those of aromatic species with formaldehyde and acetaldehyde estimated to be the most abundant VOCs in the PTR-MS mass spectrum at all engine loads. The relative abundances of benzene and toluene increased with engine load indicating their pyrogenic origin. The relative abundance of alkanes, aromatics, aldehydes and alcohols was broadly consistent with literature publications of diesel exhaust analysis by gas chromatography. About 75% of the organic ion signal could be assigned. On-line analysis of diesel exhaust using this technology may be valuable tool for diesel engine emission research.

Keywords: VOC; Hydrocarbons; PTR-MS; Diesel exhaust; Chemical ionization; Proton transfer

1. Introduction

Diesel and gasoline engines are important sources of nitrogen oxides, hydrocarbons and fine particulate matter in the urban atmosphere and have major impacts on air quality and human health. In the US, new regulations are being phased in over the next several years to significantly reduce particle emissions from diesel engines. Particle mass emissions rates and composition from diesel engines are determined by a number of factors including engine technology, engine load, air to fuel ratio, fuel parameters, exhaust temperature and driving conditions [1–4]. To reduce particle emissions, diesel exhaust aftertreatment devices are being developed. One such device is the wall flow particulate filter, whereby particles are trapped on the surface of a porous ceramic material and periodically "burned off" through a process known as regeneration [5]. The kinetics of the regeneration process and how adsorbed hydrocarbons on the particles influence the oxidation process is an active area of research [6]. Understanding the performance of these devices requires on-line monitoring of exhaust gases and particles of sufficient time resolution to relate changes in gas and particulate matter composition to changes in engine operating conditions. This paper presents results of on-line gas phase hydrocarbon analysis in

* Corresponding author. Tel.: +1 303 372 6063; fax: +1 303 372 6168.
E-mail addresses: tom.jobson@pnl.gov (B.T. Jobson), michael.alexander@pnl.gov (M.L. Alexander), gary.maupin@pnl.gov (G.D. Maupin), george.muntean@pnl.gov (G.G. Muntean).

1387-3806/$ – see front matter © 2005 Elsevier B.V. All rights reserved.
doi:10.1016/j.ijms.2005.05.009

diesel exhaust by proton transfer reaction mass spectrometry (PTR-MS). This technology was developed by Lindinger and co-workers [7,8] and has seen growing use as tool for organic trace gas monitoring in a variety of applications. The purpose of this study was to evaluate its utility in quantifying components of diesel exhaust on-line in support of diesel exhaust after treatment device research. Complex mixture analysis by this technique can not provide resolution of individual constituents to the same degree as gas chromatography based analyses, but may be the best quantitative technique to date for providing on-line, high time resolution information on selected organic species such as aromatics and light oxygenates. Smith et al. [9] have recently reported the use of a similar technique, selected ion flow tube mass spectrometry, for the on-line analysis of diesel exhaust.

2. Experimental

The PTR-MS instrument (Ionicon Analytik, Austria) continuously measures organic gases in air by H_3O^+ chemical ionization in an ion drift tube. The hydronium ion is unreactive with some major constituents of exhaust such as CO, NO, acetylene, ethene and light alkanes but does react with a broad range of organics in a non-dissociative proton transfer reaction, producing protonated product ions (RH^+) from the parent organic, shown as reaction (1):

$$H_3O^+ + R \rightarrow RH^+ + H_2O \quad (1)$$

A large number of species also fragment upon protonation, complicating the interpretation of the mass spectrum for mixtures. Under pseudo first-order reaction conditions the number density of an organic species R in the drift is given by:

$$[R] = \frac{1}{kt}\left(\frac{RH^+}{H_3O^+}\right)\frac{\varepsilon_{H_3O^+}}{\varepsilon_{RH^+}} \quad (2)$$

where H_3O^+ and RH^+ are the measured count rates of the reagent ion and protonated organic, k the ion–molecule reaction rate coefficient, t the ion drift time of H_3O^+ (reaction time) and ε is the relative transmission efficiency of the ion. The drift time can be calculated from the ion drift conditions [10,11] and the relative transmission efficiencies are determined experimentally. Given that ion–molecule reaction rate constants for exothermic proton transfer reactions occur at the collisional limit [12], the developers of this technology have stipulated that the relevant collision rate coefficients can be calculated from theory [13] or taken from experimentally determined values in the literature. A reasonable estimate of species concentrations can be determined in the absence of specific hydrocarbon calibration standards through use of Eq. (2) [7], though there have been few reports comparing measured and calculated sensitivities. Eq. (2) is appealing if reliable standards are not available.

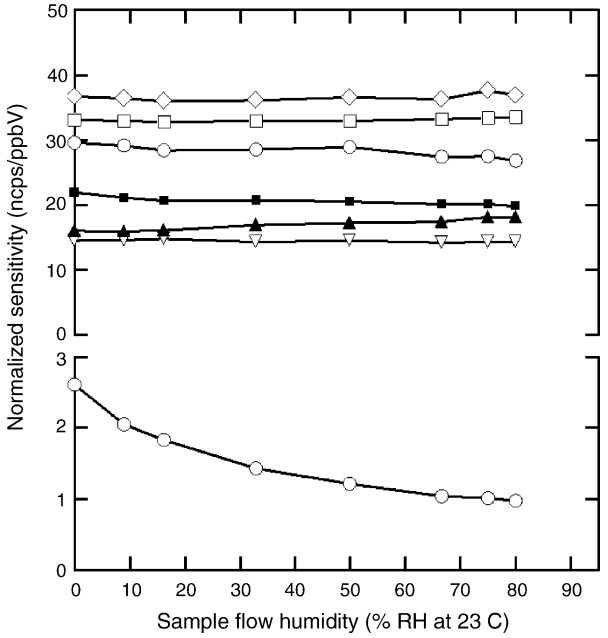

Fig. 1. Normalized sensitivity as a function of sample flow relative humidity. Upper panel shows acetone (diamonds), acetonitrile (squares), 1,2,4-trimethylbenzene (circles), benzene (filled squares), isoprene (filled triangles) and methanol (open triangles). Lower panel shows HCN on a different abscissa scale range.

A potential issue in a comparison of measured and calculated sensitivity is the presence of the water cluster ion $H^+(H_2O)_2$, which is in equilibrium with H_3O^+ in the ion drift tube. Water is always present in the drift tube due to leakage from the ion source and to the presence of humidity in the sample flow. The water cluster distribution varies with sample flow humidity, buffer gas number density in the drift (N) and applied electric field (E). The proton affinity of $H^+(H_2O)_2$ has been calculated to be 830 kJ/mol [14] making the proton transfer reaction endothermic for many hydrocarbons including most aromatics found in vehicle exhaust and urban air. Evidence of the influence of $H^+(H_2O)_2$ reactions with organics in the PTR-MS comes from studies by Warneke et al. [15] who reported humidity dependent sensitivities for several species when the drift was operated at lower field strengths (E/N).

For the conditions of our experiment we operated the PTR-MS in a regime where sensitivities are reasonably humidity independent for most species, the known exceptions being HCHO and HCN which have PA's only slightly greater than H_2O. Fig. 1 illustrates the normalized sensitivity of several hydrocarbons as a function of sample flow humidity from 0 to 80% RH at 23 °C. Drift conditions were similar to those used in the diesel exhaust sampling: 2.1 mbar drift pressure, $150T_d$ field strength and 50 °C drift tube temperature. Following the example of Warneke et al. [15], the hydrocarbon sensitivity (cps/ppbv) was normalized to per million H_3O^+ counts rates (ncps/ppbv) to account for variations in H_3O^+. A multicomponent compressed gas standard (Apel-Reimer Environmental, USA) was used to generate

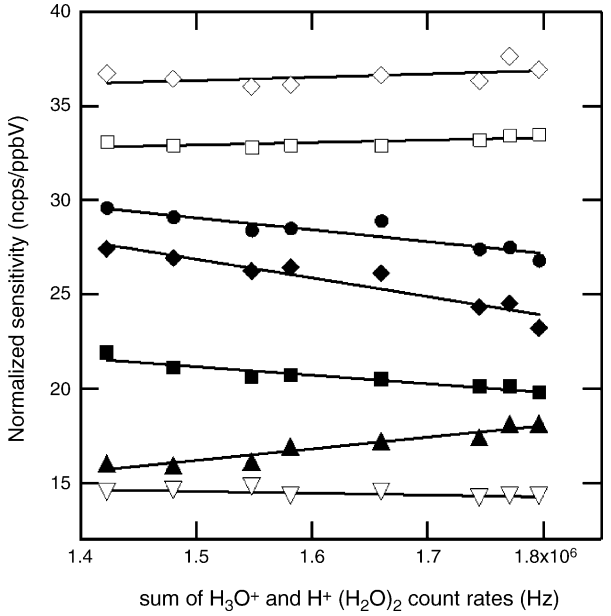

Fig. 2. Normalized sensitivity versus the sum of H_3O^+ and $H^+(H_2O)_2$ count rates showing acetone (open diamonds), acetonitrile (open squares), 1,2,4-trimethylbenzene (filled circles), toluene (filled diamonds), benzene (filled squares), isoprene (filled triangles), methanol (open triangles).

a constant sample flow of VOCs at ~40 ppbv mixing ratio level. A permeation device (VICI Metronics) was used to generate a constant mixing ratio of HCN, which was co-added to the sample stream. HCN displayed a significant dependence on humidity. For the other VOCs, the humidity dependence was less pronounced but clearly dependent on the sum of H_3O^+ and $H^+(H_2O)_2$ count rates. Fig. 2 illustrates that normalized sensitivities decreased for aromatics, increased for isoprene, while oxygenated sensitivities were reasonably independent of the summed water cluster count rates. To explain the decrease in aromatic sensitivity with increasing humidity, H_3O^+ must be decreasing in the drift, contrary to the measured 6% increase in H_3O^+ count rates. The fidelity of the water cluster ion sampling by the PTR-MS instrument has been questioned previously [15,16]. Discrepancies between measured and calculated water cluster ion ratios indicate that H_3O^+ is formed in the collision induced dissociation of $H^+(H_2O)_2$ in the ion optics transfer region between the exit orifice of the ion drift tube and the entrance orifice of the mass spectrometer [15,16]. In contrast to the aromatics, the normalized sensitivity for acetonitrile and the oxygenated species did not display a significant change with increasing humidity, while isoprene's normalized sensitivity increased, despite the inferred decrease of H_3O^+ concentration in the drift. The behavior of the oxygenates and acetonitrile is consistent with these species undergoing fast ligand switching reactions with $H^+(H_2O)_2$ with subsequent collisional dissociation of the complex into RH^+ product ions, shown as reactions (3) and (4). Molecules with weak dipole moments apparently do not undergo efficient ligand switching reactions [17] so for molecules like benzene, toluene and isoprene reaction (3) is likely unimportant. The increase in the isoprene sensitivity is consistent with direct proton transfer reaction with $H^+(H_2O)_2$—reaction (5). In our experiment, isoprene was the only molecule examined with a proton affinity greater than $H^+(H_2O)_2$, thus it can react with both H_3O^+ and $H^+(H_2O)_2$ in direct proton transfer reactions.

$$H^+(H_2O)_2 + R \rightarrow H^+(R)H_2O + H_2O \quad \text{ligand switching} \tag{3}$$

$$H^+(R)H_2O + M \rightarrow RH^+ + H_2O + M \quad \text{collisional dissociation} \tag{4}$$

$$H^+(H_2O)_2 + R \rightarrow RH^+ + H_2O \cdot H_2O \quad \text{proton transfer} \tag{5}$$

The additional production of RH^+ ions via reactions (4) and (5) would complicate comparisons of measured and calculated sensitivities based on Eq. (2).

Interestingly, Midey et al. [18] reported SIFT-MS studies showing that $H^+(H_2O)_2$ reacts with toluene, ethylbenzene and *n*-propylbenzene to yield protonated product ions (RH^+) with reaction rate constants close to the collisional limit even though the reactions are endothermic. The reaction endothermicity may have been overcome by the internal energy of the reactants [18], an important consideration for the PTR-MS where the translational kinetic energy of drifting ions has been shown to drive endothermic reactions [19]. The reaction kinetics in the PTR-MS may thus be complex and may not be well represented by Eq. (2) for all compounds and drift conditions.

For the diesel exhaust sampling experiments the PTR-MS was operated using the same drift conditions noted previously. H_3O^+ ion count rates were ~4.0×10^6 Hz corrected for transmission. The first water cluster $H^+(H_2O)_2$ was ~20% of the reagent ion signal for room air and engine idle conditions, increasing to 35% for the highest engine load experiments. This change in water cluster distribution will have only a minor influence on the relative VOC sensitivities for the different engine load conditions and therefore no corrections were applied. Calibration sensitivities (cps/ppbv) were measured during and after the experiment and compared with calculated sensitivities from Eq. (2). These results are shown in Table 1. After the diesel exhaust sampling experiment the PTR-MS was returned to the lab where the ion optics was retuned and the transmission curve measured. The retuning resulted in much less declustering of $H^+(H_2O)_2$ to H_3O^+ in the ion transfer optics and normalized sensitivities for aromatics no longer decreased with increasing humidity as was illustrated in Fig. 2. The sensitivity of the PTR-MS in the diesel exhaust sampling tests was determined from a multipoint calibration by dynamically diluting a multicomponent calibration mixture (Apel-Reimer Environmental) in humid zero air (~40% RH). The post exhaust sampling calibrations performed in the laboratory used ultra clean nitrogen at three different humidities as the diluent. The gas standard had a

Table 1
Ratio of measured to calculated sensitivity[a]

	Diesel test	Laboratory calibrations		
	Air 40% RH	Dry N_2[b]	N_2 46% RH	N_2 75% RH
Methanol	1.75	1.22 ± 0.04	1.44	1.62
Acetonitrile	1.44	1.22 ± 0.06	1.29	1.50
Acetaldehyde	1.18	1.06 ± 0.04	1.07	1.26
Acetone	1.81	1.43 ± 0.06	1.43	1.86
Isoprene	1.27	1.01 ± 0.04	1.07	1.24
2-butanone	1.81	1.37 ± 0.08	1.42	1.66
Benzene	1.33	1.00 ± 0.04	0.96	1.04
Toluene	1.49	0.96 ± 0.03	0.96	1.08
p-Xylene	1.47	0.96 ± 0.03	0.96	1.12
1,2,4-Trimethylbenzene	1.47	0.88 ± 0.02	0.86	1.05
Alpha pinene	1.29	0.93 ± 0.03	0.94	1.13

[a] Thermal rate constants calculated from Su [13].
[b] Average of three determinations.

stated accuracy of ±2% for hydrocarbons and ±5% for oxygenated species. Calculated sensitivities used collisional rate coefficients calculated from the parameterized trajectory formulation of Su [13] at the thermal temperature of the drift tube. The center of mass kinetic energy KE_{cm} of reaction (1) [20] ranged between 0.22 (methanol) and 0.29 eV (alpha pinene). Given these ion energies, using thermal rate constants for polar species such as the oxygenates and acetonitrile are at best an approximation. Values for dipole moments and polarizability were taken from Zhao and Zhang [21]. The calibration sensitivities performed after retuning and measuring the transmission curve agreed very well with calculated sensitivities for the non-polar species under dry conditions. Measured sensitivities for acetonitrile and oxygenated species ranged between ranged between a factor of 1.1 (acetaldehyde) and 1.4 (acetone) higher than calculated sensitivities for dry conditions. Measured sensitivities increased with humidity. At 75% relative humidity the measured acetone sensitivity was a factor of 1.9 greater than the calculated sensitivity. Isoprene also displayed a humidity dependent sensitivity, consistent with protonation via reaction (5). The level of agreement between measured and calculated sensitivities for the diesel exhaust sampling calibration was not as good as the laboratory based calibrations. This may be due to unknown changes in the transmission curve caused by transport of the instrument to the exhaust sampling test facility. For terpenes and aromatic species the measured to calculated sensitivity ratios ranged between 1.3 and 1.5, while for the acetonitrile and oxygenated species the measured to calculated sensitivity ratio ranged between 1.2 and 1.8.

It is not clear why the oxygenated species and acetonitrile displayed a significantly higher measured to calculated sensitivity ratio than the aromatics. Oxygenated species such as methanol are known to be lost in compressed gas cylinders. However, the concentrations of methanol and acetone in our cylinder were verified against permeation sources (VICI Metronics) and so cylinder losses cannot explain our data for these species. Calculating instrument sensitivities from Eq. (2) appears to work well for non-polar compounds such as aromatics and isoprene. However, given the above sensitivity discrepancies for polar species, their humidity dependent sensitivities and potential instrument sensitivity changes caused by changes in ion transmission, external calibration standards are warranted.

Diesel exhaust from a 4 kW diesel generator was monitored. Exhaust gas passed through a cordierite particulate filter. The majority of the exhaust flow was vented outside of the building with a portion passing through two ejection type diluters (DI-1000, Dekati Ltd., Finland) placed in series to dilute the exhaust by ∼70:1with dry ultra-zero grade nitrogen. The exact dilution ratio is uncertain and can be affected by changes in the exhaust gas temperature as engine load changes. The particulate filter and first diluter were thermostated at 200 °C. A diaphragm pump pulled 3 l-min of the diluted exhaust through 2.5-m of 1/4 in. PFA tubing at ambient temperature to the PTR-MS and this flow was subsampled at 100 ml/min into the instrument. Sampling lines on the PTR-MS were thermostated to 80 °C. A small exhaust flow from the generator was sampled directly by a smoke meter to measure soot concentration upstream of the soot filter. Mass scans were made on diesel exhaust from 20 to 210 amu with 0.5 s dwell times. Thus, it took about 1.6 min to perform a mass scan. Background PTR-MS mass scans over the same mass range were performed periodically using zero air generated by passing room air through a Pt-alumina catalyst trap heated to 300 °C. The catalyst removed hydrocarbons from the ambient air and allowed monitoring of instrument background to check for possible contamination of instrument sampling lines and the drift tube due to high hydrocarbon concentrations in the exhaust. Average background count rates were subtracted from the diesel exhaust data. No major contamination of the instrument was observed.

The diesel generator was operated at 4 load settings: 0% (idle), 20%, 40% and 80% load. About 20 mass scans were done at each load. A low sulfur diesel fuel, 0.016% S by weight percent, (Specified Fuels and Chemicals LLC, CARB Diesel HF128) was used. The fuel composition was certified to be 90% by volume of saturated compounds (i.e. *n*-alkanes, *iso*-alkanes), approximately 9% aromatic species including polycyclic aromatic compounds, and about 1% alkenes.

In addition to the exhaust sampling, a series of experiments were performed to measure the ion products of H_3O^+ reactions with C_8–C_{16} *n*-alkanes and C_8–C_{13} 1-alkenes to aid the interpretation of the exhaust gas mass spectrum. These experiments used the same ion drift conditions as in the exhaust sampling. Vapor from pure compounds was sampled into the PTR-MS by the following means. About 5 ml of compound was placed in a stainless steel vial and attached to a 1/4 in. OD SS tube. The 1/4 in. tube had an extruded end with a 400 um orifice hole allowing vapor to diffuse at a controlled rate from the vial. The vapor was diluted either with dry nitrogen or dry air. The PTR-MS sub sampled from this flow. The vial, diffusion tubing and dilution tee were placed in an enclosure and thermostated to 60 ± 2 °C. The sampling

lines from the enclosure to the PTR-MS were heated traced to 80 °C. For hexadecane and tridecane the orifice tubing was replaced with a short piece of tubing with an i.d. of ~3 mm. The apparatus produced a continuous flow of vapor at a mixing ratio that was dependent on the compounds vapor pressure.

3. Results and discussion

Exhaust emissions from diesel vehicles are a complex mixture of unburned fuel components and partially oxidized species created in combustion [22]. Diesel fuel is typically composed of organics in the molecular weight range between C_9 and C_{26} *n*-alkanes, with a large fraction of the mass between C_{12} and C_{18} [23]. Major components of the fuel mass are *n*-alkanes. There are few comprehensive studies of speciated gas phase diesel exhaust emissions. Two noteworthy studies by Siegl et al. [22] and Schauer et al. [24] reported on a broad range of volatile and semivolatile hydrocarbons including oxygenated species. The results reported from those two studies will be used as a guide to interpreting the PTR-MS mass spectra. A summary of their results is given in Table 2 showing emissions by functional group and a partial list of individual organic species that dominated group emission rates. The major functional groups found in diesel exhaust were alkanes, light alkenes, aldehydes, aromatics and ketones. Mass emission rates were dominated by light aldehydes in both cases.

Table 2
Reported diesel exhaust mass emissions rates

Organic group	Siegl et al. [22]		Schauer et al. [24]	
	mg/km	Percent of group composition	mg/km	Percent of group composition
Σ Alkanes	7.1		23	
Σ Alkenes and alkynes	12.9		17	
Ethene	9.9	77	8.6	51
Propene	1.8	14	0.8	5
Acetylene			4.6	27
Σ Aliphatic aldehydes	15.4		129	
Formaldehyde	9.2	60	22	17
Acetaldehyde	3.5	23	42	33
Propanal	0.9	6	14	11
Σ C_5–C_9 aldehydes			13	10
Σ Aromatics	9.7		15.7	
Benzene	1.0	10	2.7	17
Toluene	0.7	7	4.0	26
C_2 benzenes	0.6	6	3.6	23
C_3 benzenes	1.1	11	2.0	13
Σ Ketones	1.8		35	
Acetone	1.8	100	22	63
2-Butanone			7.5	21
Σ Alkylcyclohexanes			2	
Σ Acids			2	

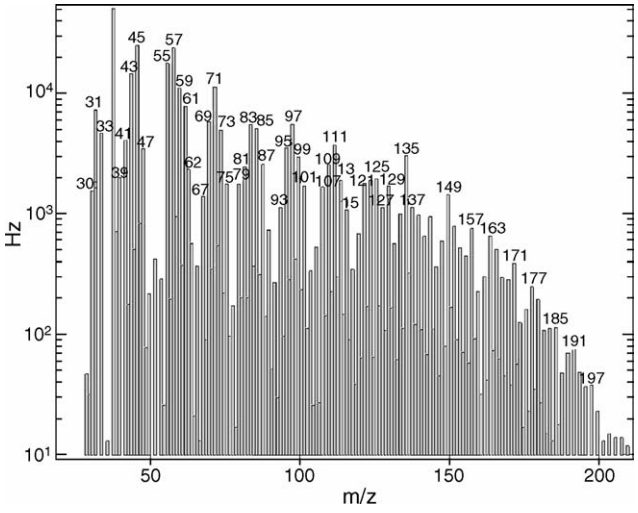

Fig. 3. PTR mass scan of diesel engine generator exhaust operating at 0% load. Ion signal intensity in counts per second (Hz) are plotted against mass to charge ratio (*m*/*z*). Background count rates have been subtracted from the spectrum. The off scale peak at $m/z = 37$ is the first hydronium ion water cluster $H^+(H_2O)_2$.

The PTR-MS mass spectrum for the engine idle condition is shown in Fig. 3. Background count rates have been subtracted; removing major ions produced in the ion source such as *m*/*z* 21, 32, 37 and 55. The mass spectrum is complex, with a peak at every mass, even numbered mass dominating. Count rates for most masses increased as engine load decreased. This is in contrast to the soot concentration, which increased with engine load. In general the mass spectra for the different loads appeared similar. Count rates of the 20 most abundant masses are shown in Table 3 and estimated mixing ratios in the diluted exhaust are given in Table 4. Mixing ratios were calculated from measured sensitivities for species listed in Table 1. The sensitivity of *p*-xylene was used as a surrogate to calculate the sensitivities of all C_2-benzene isomers (xylenes and ethylbenzene). Likewise, the sensitivity of 1,2,4-trimethylbenzene was used as a surrogate to calculate the sensitivity of all C_3-benzene isomers (trimethylbenzenes isomers, ethyl toluene isomers, etc.). The sensitivity for other aromatics was referenced to the *p*-xylene sensitivity multiplied by the ratio of the collisional rate coefficients and the ratio of relative ion transmission efficiency to account for differences in reactivity and transmission. In a likewise manner the sensitivity for C_5–C_9 aldehydes was referenced to the acetaldehyde sensitivity, and the sensitivity of cresols and dimethylphenols was referenced to the phenol sensitivity. The phenol sensitivity was determined with a permeation device (VICI Metronics) and was measured to be 1.3 times the toluene sensitivity in humid (50% RH) zero air. We assumed the formaldehyde sensitivity would be similar to that of HCN since they have similar proton affinities and therefore the back reaction of the protonated product to H_2O will be important, reducing the sensitivity implied by Eq. (2). The humidity of the sample air was not measured so for simplicity we used the HCN normalized sensitivity at 50% RH (1.3 ncps/ppbv)

Table 3
Most abundant organic ions relative to *m*/*z* 57 observed in PTR-MS spectra of diesel exhaust at different engine loads

Ion (*m*/*z*)	Peak assignment	Ion abundance relative to m57 (%)			
		Idle	20% Load	40% Load	80% Load
45	Acetaldehyde	104	107	101	85
57	C_4H_9 alkane fragment	100	100	100	100
43	C_3H_7 alkane fragment	61	64	65	79
71	C_5H_{11} alkane fragment	47	47	43	31
59	Acetone/propanal	46	46	45	28
61	Acetic acid	32	42	43	41
31	Formaldehyde	30	32	33	46
69	C_5H_9 *n*-aldehyde fragment	24	23	22	19
97	C_7H_{13} *n*-aldehyde fragment	23	23	25	16
83	C_6H_{11} *n*-aldehyde fragment	23	22	22	11
85	C_6H_{13} alkane fragment	21	21	19	8.6
73	Butanal/butanone	21	22	22	16
33	Methanol	20	20	18	20
41	Alkane fragment	17	17	17	30
111	*n*-Aldehyde fragment	16	15	15	5
95	Phenol	15	14	12	8.6
47		14	17	21	17
135	C_4 benzenes	13	12	12	3
99	C_7H_{15} alkane fragment	12	13	16	14
87		11	11	9	3.0
109	Cresols	11	10	9.1	5.1
81		10	9.1	7.1	4.2
62		10	13	17	32
125		8.2	8.0	7.7	2.2
123	Dimethylphenols/benzoic acid	7.9	7.8	8.0	5.4
113	Alkane fragment	7.9	7.4	6.7	2.2
121	C_3 benzenes	7.5	7.4	7.5	3.8
75		7.4	7.6	5.5	1.4
79	Benzene	7.3	8.3	9.6	18
101		7.1	7.1	6.2	1.6
129	Naphthalene	7.1	7.1	6.8	5.4
107	C_2 benzenes	6.9	7.1	7.2	7.0
149	C_5 benzenes	6.0	5.8	7.3	6.4
67		5.8	5.5	4.0	4.8
93	Toluene	4.7	4.7	6.1	9.9

as a proxy for the formaldehyde sensitivity. The sensitivity used for the alkanes is explained in the alkane discussion. An explanation of the mass assignments with respect to the major groups and species listed in Table 2 is given below.

3.1. Mass assignment

3.1.1. Alkanes

Analysis of medium duty diesel engine exhaust by gas chromatography has shown that *n*-alkanes and *iso*-alkanes are major gas phase constituents [22,24]. Gas phase concentrations of *n*-alkanes >C_{13} measured by Siegl et al. [22] dropped off dramatically, presumably due to diminishing abundance in the fuel and increased gas-to-particle partitioning of heavier alkanes. Similarly, Schauer et al. [24] observed gas phase *n*-alkanes concentrations decreased for species >C_{18} as shown in Fig. 6. Differences between the studies may reflect the higher relative concentrations of heavier alkanes in the diesel duel used by Schauer et al. [24].

The proton affinity for light alkanes (<C_4) is known to be less than that of water [25] thus these species are not measurable with the PTR-MS instrument. The proton affinities of larger alkanes are unknown and it is not clear if the PTR-MS would be sensitive to the alkanes found in diesel exhaust. A SIFT-MS study by Arnold et al. [26] concluded that while H_3O^+ + alkane proton transfer reactions for alkanes larger that that of hexane should be exothermic, the reactions proceeded at a fraction of the collisional limit and no direct proton transfer products were observed. Dominant products were alkyl cation fragments and association product ions ($R{\cdot}H_3O^+$), with association being the dominant reaction channel at 300 K. The alkyl cation fragments were assumed to occur as a result of dissociative proton transfer, and the reaction rate increased with *n*-alkane carbon number. The protonation of dodecane was measured to be ∼20% of the collisional limit at 300 K [26]. Other ion flow tube studies of the H_3O^+ reaction with *n*-alkanes have reported that *n*-alkanes >C_{10} react with H_3O^+ near the collisional limit to form only association product ions [27].

We conducted separate studies examining the PTR-MS mass spectrum of C_8–C_{13} alkanes, hexadecane and *n*-butylcyclohexane. Spectra were obtained using both N_2 and

Table 4
Estimated mixing ratios (ppbV) of organics in diluted diesel exhaust at different engine loads

	Mass (*m*/*z*)	Engine load			
		0%	20%	40%	80%
Σ Alkanes >C_{10}	41, 43, 57, 71, 85, 99	3731	2821	1225	783
Σ Aldehydes and ketones		2180	1710	733	595
Formaldehyde	31	1224	973	431	439
Acetaldehyde	45	426	334	133	81
Acetone/propanal	59	132	101	41	18
2-Butanone/butanal	73	59	47	20	10
Σ C_5–C_9 aldehydes	69, 83, 97, 111	340	255	107	46
Σ Aromatics		439	337	152	86
Benzene	79	47	40	20	27
Toluene	93	25	19	11	12
C_2-benzenes	107	39	30	13	9
C_3-benzenes	121	45	34	15	5
C_4-benzenes	135	85	64	25	5
C_5-benzenes	149	45	33	17	11
C_6-benzenes	163	21	17	7	2
Naphthalene	129	44	34	14	8
Methylnapthalenes	143	27	22	10	1
Dimethylnaphtahlenes	157	24	20	10	1
Trimethylnaphthalenes	171	12	9	5	1
Fluorene	167	9	7	3	0.6
Acenaphthene	153	15	10	3	0.7
Σ Alcohols		228	172	66	38
Methanol	33	81	63	24	19
Phenol	95	60	45	17	8
Cresols	109	49	36	13	5
Dimethylphenols	123	37	28	12	6

air as a matrix. N_2 was used to reduce O_2^+ concentrations in the drift to below 0.02% of H_3O^+ count rates. O_2^+ is produced by the PTR-MS ion source when sampling air; typical O_2^+ number densities in our exhaust sampling experiment were 3% of H_3O^+. O_2^+ is known to react with alkanes at the collisional limit in a dissociative charge transfer reaction [27]. The influence of the O_2^+ reaction was tested by comparing the ion signal strength observed between an N_2 and air matrix mass spectra of decane. No significant differences were observed, implying that *n*-alkanes were reacting rapidly with H_3O^+. Fig. 4 illustrates the background subtracted spectra for *n*-octane, *n*-dodecane and *n*-hexadecane in dry N_2. The dominant products ions were *m*/*z* 41 and 14*n* + 1 alkyl cations (*n* = 3, . . ., 8). No direct proton transfer product ion was observed, similar to the SIFT-MS studies. Only a weak ion signal for the $R{\cdot}H_3O^+$ association product was observed (∼1% of *m*/*z* 57). Interestingly, the ion signal at *m*/*z* 37, corresponding to $H^+(H_2O)_2$, was elevated in many of the spectra, suggesting that the $R{\cdot}H_3O^+$ ion product may also be undergoing rapid ligand switching reactions with H_2O molecules to form $H^+(H_2O)_2$ [27].

$$R \cdot H_3O^+ + H_2O \rightarrow H^+(H_2O)_2 + R \quad (6)$$

Fig. 5 compares the relative abundance of the 14*n* + 1 masses for the *n*-alkanes and a reference electron impact mass spectrum of *n*-tridecane to show the similarity to the PTR-MS fragmentation pattern. For comparison the ion signal at these masses in the diesel exhaust mass spectra are also shown. The relative abundance of the 14*n* + 1 peaks in the exhaust samples diminished more gradually at higher masses than the *n*-alkane mass spectra. One reason for this might be the presence of branched alkanes. By analogy with the *n*-alkanes and the similarity of their product fragments to those observed from electron impact, the branched alkanes also likely react with H_3O^+ in dissociative proton transfer reactions, fragmenting to similar ion products as the *n*-alkanes. The relative intensity of the 14*n* + 1 mass fragments for *iso*-alkanes ionized by electron impact varies depending on molecular structure [28]. The relative large ion signals at *m*/*z* 99, 113, 127 observed in the exhaust samples may be due to branched alkanes, which are known to be a significant component of diesel fuel.

Fig. 6 shows the relative *n*-alkane fuel composition reported by Siegl et al. [22] and Schauer et al. [24] and, the gas phase emissions rates from Schauer et al. [24], along with measured *n*-alkane protonation efficiencies by Arnold et al. [26]. Gas phase mass emission rates from Schauer were dominated by light alkanes (<C_7) with a broad secondary peak centered around hexadecane (C_{16}). Gas phase emissions rates of higher alkanes likely arise from unburnt fuel. The PTR-MS is insensitive to the light alkanes (<C_7) where protonation efficiencies are less than 2.5% of the collisional rate but increase to ∼20% for decane [26]. We conclude that the PTR-MS was likely responding to C_{10}–C_{20} alkanes and *iso*-alkanes present in diesel exhaust, giving rise to significant signals at *m*/*z* 41, 43, 57, 71, 85 and 99. The sum of these ion

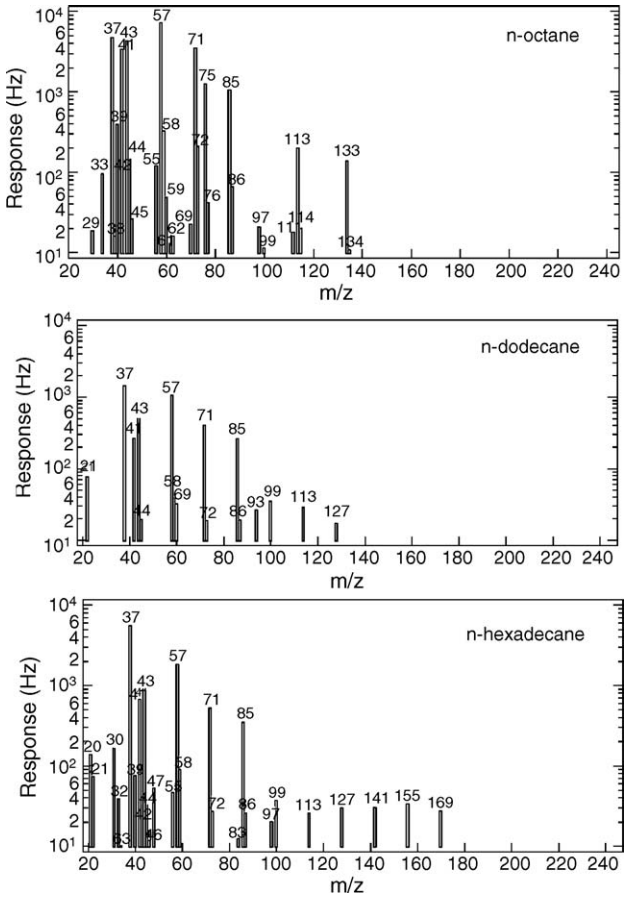

Fig. 4. Ion products of the reaction of H_3O^+ with a series of *n*-alkanes in dry N_2.

signals may be useful for estimating total gas phase alkane emissions from unburnt fuel (C_{10}–C_{20} range). To quantify these emission rates more studies are required to determine how rapidly the proton transfer reaction increases for alkanes >C_{10}. For the purpose of this study, we assumed a rate coefficient equal to 50% of the *n*-decane collisional rate to represent the alkane group dissociative proton transfer reaction probability with H_3O^+ and used Eq. (2) to estimate mixing ratios. While the calculated alkane mixing ratios are highly uncertain, they provide a provisional estimate to compare with other compound classes and to note trends at different engine load conditions.

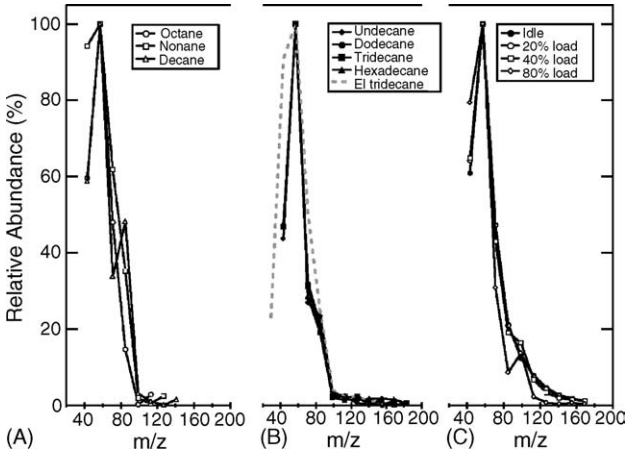

Fig. 5. Abundance of $14n+1$ peaks relative to *m*/*z* 57 observed for (A) C_8–C_{10} *n*-alkane, (B) C_{11}–C_{16} *n*-alkane compared with tridecane EI mass spectrum (dashed line) (C) diesel exhaust at various engine loads.

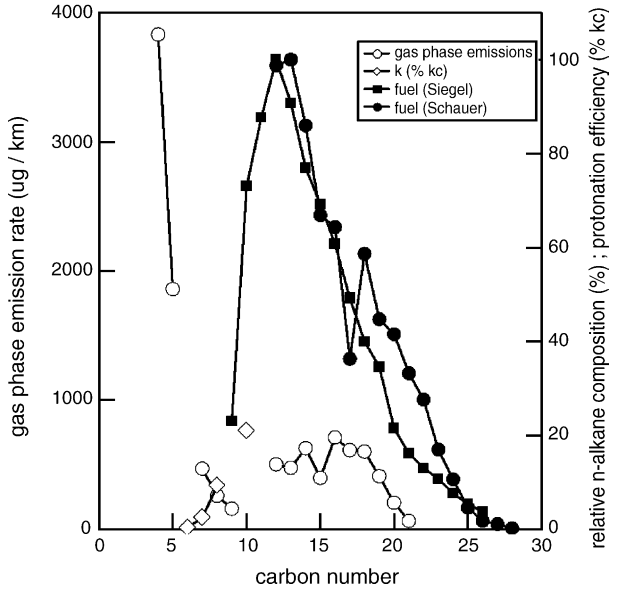

Fig. 6. Relative emission rates of gas phase *n*-alkanes in diesel exhaust (open circles) compared with relative abundance in diesel fuel (filled circles and squares), and estimated proton transfer reaction efficiency of H_3O^+ + alkane reactions (diamonds). See text for references to data.

The PTR mass spectrum of *n*-butylcyclohexane was also obtained and the product ion distribution was found to be similar to the electron impact mass spectra, with the dominant peak at *m*/*z* 83 and significant peaks at *m*/*z* 57, 97 and 137. The ions at *m*/*z* 83 and 97 correspond to fragments resulting from cleavage of the alky group from the cyclohexane ring ($C_6H_{11}^+$) and cleavage of the alkyl group yielding a $C_7C_{13}^+$ cation containing the cyclohexane ring. The *m*/*z* 83 and 97 signals were prominent in the PTR-MS mass scans of diesel exhaust at all engine loads. However, Schauer et al. [24] report that alkylcyclohexanes comprise only about 2% of the fuel mass relative to alkanes, and likewise were a minor component of exhaust emissions. The high mass signals at *m*/*z* 83 and 97 appeared to be inconsistent with the presence of alkylcyclohexanes and may have been dominated by fragments from other types of species such as *n*-aldehydes.

3.1.2. Alkenes and alkynes

The emissions of ethene, propene and acetylene are reportedly a significant mass fraction of the total hydrocarbon emissions from diesel engine exhaust [22,24]. The proton affinities of ethene and acetylene are less than that of H_2O and thus not detectable by H_3O^+ chemical ionization. SIFT-MS studies have shown that small alkenes (C_3–C_5) are known to produce predominantly RH^+ ion products upon reaction

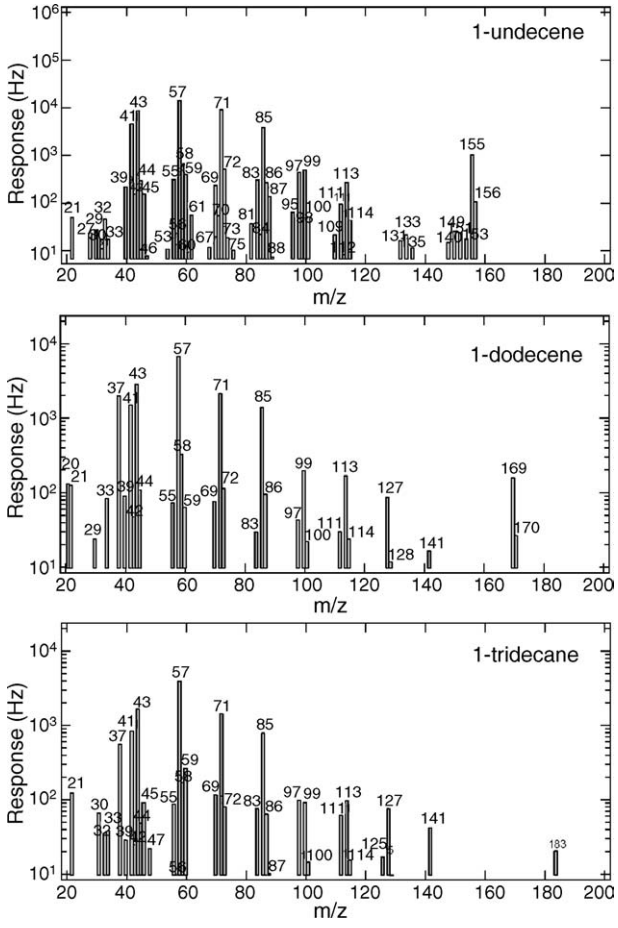

Fig. 7. Ion products of the reaction of H_3O^+ with a series of 1-alkenes in dry N_2.

with H_3O^+ while larger alkenes display significant dissociation [29]. We obtained mass spectra for C_8–C_{13} 1-alkenes to establish their fragmentation behavior in the PTR-MS. Fig. 7 shows representative spectra for several 1-alkenes. While an RH^+ product ion was apparent, the dominant ion products were a series of alkyl cation fragment ions similar to those observed for alkanes. The more extensive fragmentation in our experiments compared to the SIFT-MS experiments [27] was likely due to the larger ion kinetic energies of the PTR-MS instrument. From the Wannier expression, the calculated kinetic energy of H_3O^+ ions was 0.35 eV, leading to center of mass kinetic energies KE_{cm} of 0.32 eV for these reactions [20]. Larger alkenes are a minor component of diesel exhaust but we note that the fragmentation of alkanes and alkenes to similar masses (*m*/*z* 41, 43, 57, 71, 85) precludes differentiating between them in exhaust analysis and furthermore prevents quantifying propene and the butene isomers.

Interestingly Smith et al. [9,30] reported high concentrations of C_3–C_6 dienes and/or cycloalkenes in their SIFT-MS analysis of diesel exhaust using H_3O^+ reagent ion chemistry. With the exception of 1,3-butadiene, large concentrations of dienes and or/cycloalkenes were not reported in diesel exhaust by Siegl et al. [22] and Schauer et al. [24]. The large ion signal in the SIFT-MS spectra at *m*/*z* 69 may be in part due to a methanol hydrate. Smith et al. [9] reported a large ion signal at *m*/*z* 81 and assigned it as C_6H_8—a hexatriene. We also observed a significant *m*/*z* 81 in our diesel exhaust mass spectra. To our knowledge there has been no reported identification of hexatrienes or cyclohexadienes as major components of diesel exhaust from gas chromatography analysis. We suspect that *m*/*z* 81 in our mass spectra is a fragment ion.

3.1.3. Aldehydes and ketones

Emissions of formaldehyde, acetaldehyde and to a lesser extent propanal are a major fraction of the mass emissions of diesel engine exhaust [22,24]. These species appear at *m*/*z* 31, 45 and 59, respectively, in the PTR-MS and indeed were observed to be major ion signals in the diesel exhaust sampling. Formaldehyde and acetaldehyde are thought to be relatively free from organic isobaric interferences and from interfering mass fragments from larger organics. Propanal is isobaric with acetone but acetone is found at higher concentrations in the exhaust [22,24]. The *m*/*z* 59 signal is thus likely a composite of propanal and acetone. Emissions of *n*-aldehydes from C_4 to C_{13} are reported to be important with a summed mass emission rate equivalent to the formaldehyde emission rate [24]. Under the ion drift conditions used here protonated *n*-aldehydes can dehydrate, dissociating into a number of fragments whose relative intensities depend on the parent aldehydes [31]. For mixture of C_5–C_9 *n*-aldehydes major mass peaks would occur at *m*/*z* 69, 73, 83 and 97 [31]. The ion product distribution of higher *n*-aldehydes is not known. The PTR-MS mass spectra of diesel exhaust displayed strong ion signals at these masses, consistent with the Schauer analysis that longer chain aldehydes are a significant component of diesel exhaust. The Smith et al. [9] study also measured high concentrations of formaldehyde and acetaldehyde in diesel exhaust, with C_3–C_5 *n*-aldehydes making a minor contribution. Emissions of aldehydes have important consequences for urban air quality due to their reactivity towards hydroxyl radical and their role as radical sources upon photolysis. Formaldehyde and acetaldehyde are also known air toxics. Further tests using more specific methods for aldehyde detection are warranted to confirm strong mass emissions rates of aldehydes from diesel exhaust.

3.1.4. Aromatics

Aromatic species are a major component of diesel exhaust. For the most part these species do not fragment under the ion drift conditions used here. A notable exception is ethylbenzene, which fragments to *m*/*z* 79 with 40% yields under our drift conditions. The PTR-MS cannot resolve geometric isomers but can quantify the sum of the isomers grouped according to molecular weight such as C_2-benzenes (C_8H_{10}), C_3-benzenes (C_9H_{12}). Given the mass resolution of the PTR-MS, isobaric interferences from species with a different molecular formula can occur. For example, if the aromatic species has the molecular formula C_xH_y then species with

formulas $C_{x-1}H_{y-4}O$ may be interferences. Two examples are known for diesel exhaust, benzaldehyde is a mass interference for C_2-benzene isomers (i.e. xylenes and ethylbenzene) and acetophenone for C_3-benzenes (i.e. trimethylbenzenes, ethyltoluenes, etc.). For polycyclic aromatic hydrocarbons there are potentially additional isobaric interferences from more saturated compounds $C_{x-1}H_{y+12}$. For example, undecane could potentially be a mass interference with dimethylnaphthalenes. Fortunately, *n*-alkanes and likely *iso*-alkanes dissociate upon reaction with H_3O^+, and interferences should be insignificant for PAHs. One way to test for mass interferences is to examine the $RH^+ + 1$ to RH^+ ion abundance ratio and relate this to expected isotopic abundance. For example, protonated benzene appears at *m*/*z* 79. A peak at *m*/*z* 80 will also appear due to benzene containing a ^{13}C or ^{2}H atom and its intensity relative to *m*/*z* 79 can be calculated from the known isotopic abundances of ^{13}C and ^{2}H. If the signals at these masses are due to benzene (or geometric isomers) then the *m*/*z* 80–79 ions signal ratio should be equal to benzene's isotopic abundance. Fig. 8 shows the measured $RH^+ + 1$ to RH^+ ratios for the engine idle condition versus expected isotope ratios for several peaks tentatively identified as aromatics, oxygenates and the mass fragments from alkanes and *n*-aldehydes noted above. In general, the level of agreement is quite good with a few notable exceptions such as benzene, toluene and trimethylnaphthalene. The trimethylnaphthalene ratio had a large uncertainty (±40%) due to the low counts rates. In contrast, the count rates for the benzene and toluene masses were quite large and the deviations from their calculated isotopic abundance are statistically significant. In the case of benzene the larger $RH^+ + 1$ abundance was likely due to fragmentation of *n*-alkylaromatics such as ethylbenzene. The large deviation suggests significant contributions from species having alkyl side groups with more than four carbon atoms ($C_{10}H_{14}$). Similarly, toluene may also be affected by fragmentation from larger di-substituted aromatics such as ethyltoluene isomers. Alternatively, the higher than expected $RH^+ + 1$ abundance for these species may also

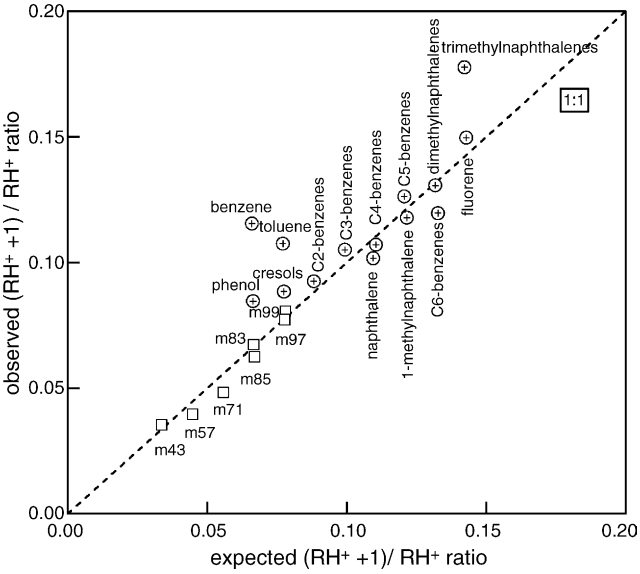

Fig. 8. Observed $(RH^+ + 1)/RH^+$ ratio vs. expected $(RH^+ + 1)/RH^+$ isotopic abundance for ions tentatively identified in the engine idle mass scans. Circles are aromatic species and squares are suspected hydrocarbon fragment ions from alkanes and *n*-aldehydes.

be due to other species at the *m*/*z* 80–94 masses such as N-containing organics like pyridine and aniline (MW = 79.04) or methylpyradine (MW = 93.13), respectively. The "excess" counts at *m*/*z* 80 would imply a pyridine mixing ratio in the exhaust of about 1.5 ppbv.

3.2. Exhaust mixing ratios and dependence on engine load

Changes in the relative hydrocarbon abundance were apparent as a function of engine load. Fig. 9 shows the ion signal intensity relative to *m*/*z* 57 representing the alkane signal from unburned diesel fuel. Benzene and toluene abundances both increased with engine load, similar to soot concentrations, indicating their pyrogenic origin. Higher molecular

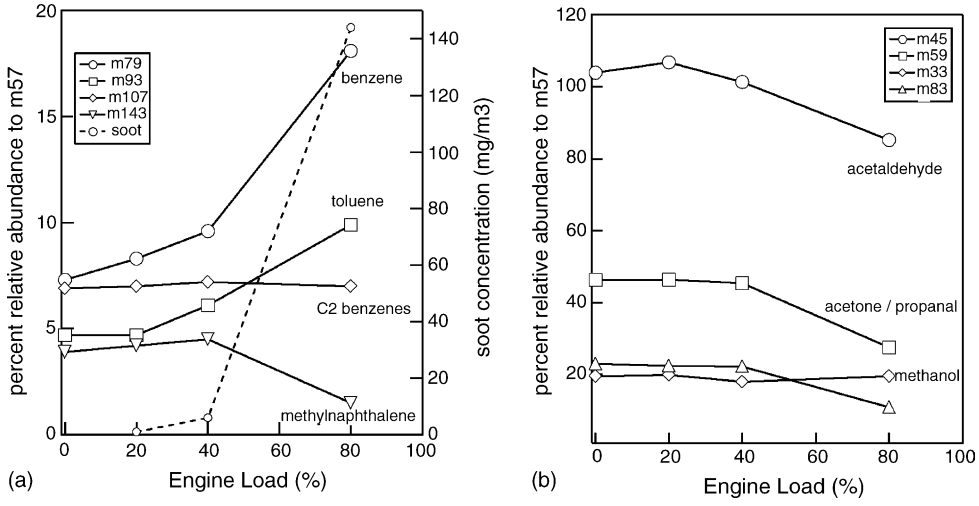

Fig. 9. Ion abundance relative to m57 as a function of engine load (A) aromatic species and soot concentration (B) oxygenated species.

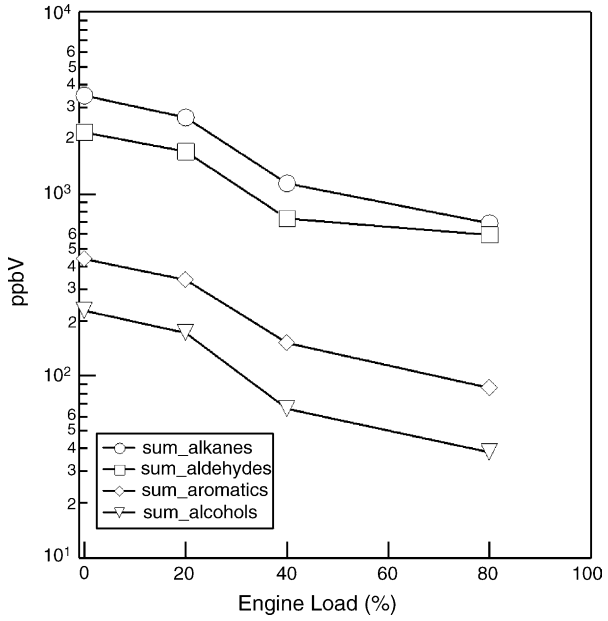

Fig. 10. Functional group mixing ratios vs. engine load. Masses associated with the different groups are shown in Table 4.

weight aromatics such as methylnaphthalene shown in the figure decreased in abundance at the highest engine load. This may indicate scavenging by the increased soot production. Aldehydes in general decreased with engine load with the exception of HCHO, while methanol displayed no change in relative abundance. Mixing ratios for most species decreased as the engine load increased. This is shown in Fig. 10 where the summed group concentrations shown in Table 4 are plotted versus engine load. Aldehyde emissions appeared to level out as the engine load decreased while alkane, aromatic and alcohol emissions decreased.

4. Conclusions

Volatile organic compounds (VOC) emitted in diesel generator exhaust were monitored on-line using a proton transfer reaction mass spectrometer (PTR-MS). The purpose of this study was to evaluate the PTR-MS as a quantitative on-line monitoring tool for engine exhaust research. Under normal operating conditions of the instrument we observed water vapor dependent sensitivities. The dependence was negative for aromatics (normalized sensitivity decreased) and positive for isoprene, while oxygenates displayed little change. This behavior implies VOC reactions with $H^+(H_2O)_2$ in the ion drift are important and that the H_3O^+ count rates were overestimated due to fragmentation of protonated water clusters following their extraction from the drift. This artifact was largely eliminated with subsequent retuning of the ion transfer optics. Under these new conditions the measured sensitivities for non-polar species agreed well with theoretical sensitivities. Measured sensitivities for polar species displayed a significant humidity dependence and were up to a factor of two greater than calculated sensitivities. These tests suggest that reactions with $H^+(H_2O)_2$ are important for understanding species dependent sensitivities of the PTR-MS instrument.

The diesel exhaust mass spectrums were complex but interpretable and allowed identification of several key species. Notably, the PTR-MS appears to respond to alkanes with carbon numbers $>C_{10.}$ These alkanes represent unburnt fuel emissions. Laboratory tests demonstrated that alkanes and 1-alkenes undergo a dissociative proton transfer reaction with H_3O^+ in the PTR-MS to produce characteristic $14n+1$ ($n=3, \ldots, 8$) ion product peaks similar to those observed under standard 70 eV electron impact. This may allow an estimate to be made of the total alkane concentration in the exhaust by summing the signals at the major alkane fragment peaks: m/z 41, 43, 57, 71, 85 and 99. However, it is unclear how rapidly H_3O^+ reacts with these alkanes. A number of aromatic constituents were also identified; major components include benzene, toluene, C_2 through C_6 substituted benzenes, naphthalene and methylnaphthalenes. Concentrations of benzene and toluene may be overestimated because of potential fragmentations from higher aromatics as evidence by deviations in their isotopic ratios. The dominant exhaust species determined by the PTR-MS were formaldehyde and acetaldehyde. There is evidence that higher *n*-aldehydes (C_5–C_9) may also have a significant presence in diesel exhaust due to large ion signals at m/z 69, 83, 97 and 111. VOC concentrations decreased as a function of engine load, but the relative abundance of several species, in particular benzene and toluene, displayed significant changes with load. The relative abundance of the major exhaust components (alkanes, aromatics, aldehydes, alcohols) as determined by the PTR-MS was broadly consistent with previously published diesel exhaust studies using gas chromatography methods. About 75% of the ion single in the PTR mass spectrum could be identified based on the assignments in Table 3. We conclude that the PTR-MS may be broadly useful for on-line monitoring of major VOC exhaust components in engine emissions studies. More studies are required to better understand H_3O^+ + alkane reaction kinetics in the PTR-MS.

Acknowledgement

Vivian White is gratefully acknowledged for her work on these experiments as part of her summer internship under the US DOE Community College Investigator Program.

References

[1] D.B. Kittelson, J. Aerosol. Sci. 29 (1998) 575.
[2] J. Yanowitz, R.L. McCormick, M.S. Graboski, Environ. Sci. Technol. 34 (2000) 729.
[3] M.P. Fraser, K. Lakshmanan, S.G. Fritz, B. Ubanwa, J. Geophys. Res. 107 (2002), doi:10.1029/2001JD000558.
[4] T.J. Alander, A.P. Leskinen, T.M. Raunemaa, L. Rantanen, Environ. Sci. Technol. 38 (2004) 2707.

[5] G.C. Koltsakis, A.M. Stamatelos, Prog. Energy Combust. Sci. 23 (1997) 1.
[6] I.P. Kandylas, A.M. Stamatelos, Ind. Eng. Chem. Res. 38 (1999) 1866.
[7] A. Hansel, A. Jordan, R. Holzinger, P. Prazeller, W. Vogel, W. Lindinger, Int. J. Mass Spectrom. Ion Processes 149/150 (1995) 609.
[8] W. Lindinger, A. Hansel, A. Jordan, Int. J. Mass Spectrom. Ion Processes 173 (1998) 191.
[9] D. Smith, P. Spanel, D. Dabill, J. Cocker, B. Rajan, Rapid Commun. Mass Spectrom. 18 (2004) 2830.
[10] D.R. Hanson, J. Greenberg, B.E. Henry, E. Kosciuch, Int. J. Mass Spectrom. 223/224 (2004) 507.
[11] J.A. de Gouw, C. Warneke, T. Karl, G. Eerdekenes, C. van der Veen, R. Fall, Int. J. Mass Spectrom. 223–224 (2003) 365.
[12] D.K. Bohme, in: P. Ausloss (Ed.), Interactions Between Ions and Molecules, Plenum Press, New York, 1975.
[13] T. Su, J. Chem. Phys. 89 (1988) 5355.
[14] Y. Kawai, S. Yamaguchi, Y. Okada, K. Takeuchi, Y. Yamauchi, S. Ozawa, H. Nakai, Chem. Phys. Lett. 377 (2003) 69.
[15] C. Warneke, C. van der Veen, S. Luxembourg, J.A. de Gouw, A. Kok, Int. J. Mass Spectrom. 207 (2001) 167.
[16] M. Steinbacher, J. Dommen, C. Ammann, C. Sprig, A. Neftel, A.S.H. Prevot, Int. J. Mass Spectrom. 239 (2004) 117.
[17] P. Spanel, D. Smith, J. Phys. Chem. 99 (1995) 15551.
[18] A.J. Midey, S. Williams, S.T. Arnold, A.A. Viggiano, J. Phys. Chem. A 106 (2002) 11726.
[19] A. Hansel, W. Singer, A. Whisthaler, M. Schwarzmann, W. Lindinger, Int. J. Mass Spectrom. Ion Processes 167/1687 (1997) 697.
[20] M. McFarland, D.L. Albritton, F.C. Fehsenfeld, E.E. Ferguson, A.L. Schmeltekopf, J. Chem. Phys. 59 (1972) 6620.
[21] J. Zhao, R. Zhang, Atmos. Environ. 38 (2004) 2177.
[22] W.O. Siegl, R.H. Hammerle, H.M. Herrmann, B.R. Wenclawiak, B. Luers-Jongen, Atmos. Environ. 33 (1999) 797.
[23] R.H. Hammerle, W.O. Siegl, H.M. Herrmann, B.W. Wenclawiak, SAE Paper No. 952353, Society of Automotive Engineers, 1995.
[24] J.J. Schauer, M.J. Kleeman, G.R. Cass, B.R.T. Simoneit, Environ. Sci. Technol. 33 (1999) 1578.
[25] E.P. Hunter, S.G. Lias, J. Phys. Chem. Ref. Data 27 (1998) 413.
[26] S.T. Arnold, A.A. Viggiano, R.A. Morris, J. Phys. Chem. A 102 (1998) 8881.
[27] P. Spanel, D. Smith, Int. J. Mass Spectrom. 181 (1998) 1.
[28] F.W. McLafferty, F. Turecek, Interpretation of Mass Spectra, fourth ed., University of Science Books, Sausalito, CA, USA, 1993.
[29] A.M. Diskin, T. Wang, D. Smith, P. Spanel, Int. J. Mass Spectrom. 218 (2002) 87.
[30] D. Smith, P. Cheng, P. Spanel, Rapid Commun. Mass Spectrom. 16 (2002) 1124.
[31] E. Boscaini, Comparison of various high sensitivity analytical methods (PTR-MS, MIMS, GC-O, SA) and application to food chemistry, Ph.D. Thesis, Leopold Franzens Universität, Innsbruck, Austria, 2002.